Quantitative characterization of optical and physiological parameters in normal breasts using time-resolved spectroscopy: *in vivo* results of 19 Singapore women

Weirong Mo
Tryphena S. S. Chan
Ling Chen
National University of Singapore
Division of Bioengineering
Faculty of Engineering
Singapore, 117574

Nanguang Chen
National University of Singapore
Faculty of Engineering
Division of Bioengineering
and
Department of Electrical and Computer Engineering
Singapore, 117576

Abstract. We report the quantitative measurements of optical and physiological parameters of normal breasts from 19 Singapore women by using time-resolved diffuse optical spectroscopy. Intrinsic absorption coefficient (μ_a) and reduced scattering coefficients (μ_s') of breasts were calculated from the time-resolved photon migration data. Physiology of breasts was characterized using the concentrations of oxyhemoglobin, deoxyhemoglobin, total hemoglobin (*THC*), and oxygenation saturation. On average, the experiment results showed that the μ_a of young women (below 40 years old) was 36 to 38% greater than that of older women (above 40 years old) and that parameter *THC* was approximately 42% greater. Results also showed that the *THC* of premenopausal women was 24.3 μMol/L, which was approximately 69% larger than that of postmenopausal women at 14.1 μMol/L. Meanwhile, the μ_a of premenopausal women was approximately 60% larger than that of postmenopausal women. Correlation analysis further showed that the optical and physiological parameters of breasts were strongly influenced by changes in the women's age, menopausal states, and body mass index. These *in vivo* experiment results will contribute to the breast tissue diagnosis between healthy and diseased breast tissues. [DOI: 10.1117/1.3257251]

Keywords: breast; breast optics; near-infrared spectroscopy; photon migration.

Paper 09233RR received Jun. 9, 2009; revised manuscript received Sep. 7, 2009; accepted for publication Sep. 8, 2009; published online Nov. 4, 2009.

1 Introduction

Near-infrared (NIR) diffuse optical spectroscopy (DOS) have been proven in the last decades as a viable noninvasive optical instrument for human breast tissue examination.[1–4] In comparison to conventional breast cancer diagnostic modalities such as x-ray mammography,[5] breast magnetic resonance imaging (MRI),[6] and breast ultrasonography,[7,8] DOS differentiates normal and diseased breast tissues by quantifying the temporal or spatial changes of tissue intrinsic properties.[9] This unique feature makes DOS a useful supplementary tool to the conventional diagnosis modalities. Other system merits, such as noninvasiveness, nonionization hazard, and noncompression of breast are also favorable for routine clinical breast examination.[4,10] Women with high breast cancer risk or dense breast tissue who may not suitable for conventional diagnostic modalities can benefit from DOS in breast tissue abnormalities examination.[3,11]

One promising DOS instrument currently under development is the time-resolved DOS, which has shown advantages on high temporal resolution, high temporal linearity, and full-spectrum information.[12] Complete spectroscopy characterization can be achieved by analyzing the time-resolved photon migration data, known as the temporal point spread functions (TPSF).[13] For system implementation, spread spectrum correlation technique is an attractive approach because it offers faster data acquisition speed as well as lightweight system structure compared to the classic time-resolved techniques, which normally involve ultrashort pulse laser and time-correlated photon count (TCSPC) devices.[13–15]

Breast cancer is the most common cancer among Singapore women. Early detection of breast cancer is crucial to reduce mortality rates. This research aims to explore the applicability of time-resolved spectroscopy for breast tissue characterization. In this article, we report the quantitative measurements of breast optical properties and physiological parameters from 19 healthy Singapore women. To the best of our knowledge, this is the first characterization of human breasts *in vivo* in this demographic population. The time-resolved DOS instrument is developed using the pseudorandom bit sequence (PRBS) correlation technique, which can acquire TPSF signals in a fast speed. Two types of informa-

Address all correspondence to: Nanguang Chen, National University of Singapore, Division of Bioengineering, Faculty of Engineering, 7 Engineering Drive 1, E1-05-19 Singapore 117576. Tel: 65-6516 4401; Fax: 65-6872 3069; E-mail: biecng@nus.edu.sg

1083-3668/2009/14(6)/064004/7/$25.00 © 2009 SPIE

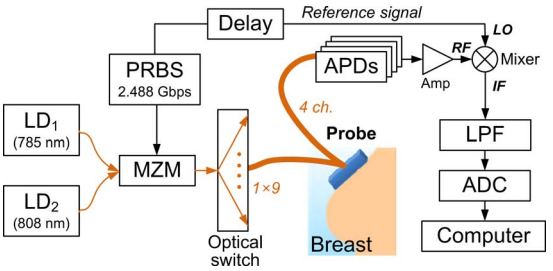

Fig. 1 Block diagram of time-resolved DOS, including two NIR laser diodes (LD_1 and LD_2), nine source fibers, and four detection fiber bundles. Amp=amplifiers. LPF=low-pass filter.

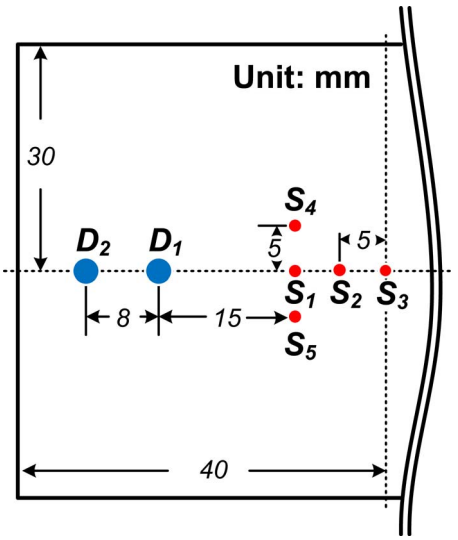

Fig. 2 Handheld probe in a reflective mode. Source fibers (small red spots) and detection fiber bundles (large blue spots) are arranged in a centrosymmetric pattern. (Color online only.)

tion are obtained from the time-resolved measurements. The first type is optical properties, specifically the absorption coefficient (μ_a) and the reduced scattering coefficient (μ_s'). The second type is physiological parameters, specifically, the concentrations of oxyhemoglobin (HbO) and deoxyhemoglobin (Hb), the total hemoglobin concentration (THC), and the oxygenation saturation (SO). This study examines the parameter characterization in association with the menopausal states and ages. We found that the value of breast optical properties (especially the μ_a) and physiological parameters (THC and SO) varied significantly between premenopausal and postmenopausal women. Meanwhile, we observed a conspicuous contrast in optical and physiological parameters between young (below 40 years old) and older women (above 40 years old). Quantitative analysis showed a high correlation between these optical/physiological parameters and the age, body mass index (BMI), and menopausal states of women.

2 Materials and Methods

2.1 *Instrument*

In our previous studies, we reported a viable time-domain diffuse optical tomography (DOT) system using PRBS correlation technique.[16] To obtain time-resolved DOS functionality, the DOT system was reconfigured and optimized. Figure 1 shows the schematic of the time-resolved DOS instrument. Briefly, two NIR laser beams at 785 nm and 808 nm alternatively went through a Mach-Zehnder modulator (MZM), in which their intensities were modulated by a train of 2.488-Gbps PRBS signal. An optical switch multiplexed the modulated light into nine source fibers. A handheld probe, which mounted all of these source fibers along with an additional four detection fiber bundles, was placed on the breast surface for probing. The optical power of 785 nm and 808 nm at the tips of the source fibers were approximately 1 mW. The source fibers sequentially delivered the excited light into the tissue and the optical reflectance from the breast was fiber-coupled to four avalanche photodiodes (APDs) through four fiber bundles. The optoelectronic conversion signals were amplified and eventually correlated with the reference PRBS signals at the mixer. The TPSF signals were extracted from the down-conversion and acquired by computer via analog-to-digital converters (ADCs). Figure 2 shows the handheld probe, which mounts nine source fibers and four fiber bundles in a centrosymmetric pattern. The source-to-detector separations range from 1.5 cm to 4.33 cm. In order to acquire system impulse response functions (IRFs) for each source–detector pair, a diffuse white paper was placed at 18 cm in front of the probe. The optical reflectance acquired by each source–detector pair was regarded as the IRFs. To figure out the fiber-coupling coefficients between fiber bundles and the corresponding APDs, phantom-based experiments were conducted to calibrate the system. The procedures for system IRF acquisition, system calibration and data accuracy assessments of TPSF have been described in detail in the previous studies.[16,17]

2.2 *Models and Assumptions*

For *in vivo* breast tissue probing, the diffusion equation is valid for modeling photon migration behaviors in the breast tissues.[18,19] Using Green's function as the analytical solution to the diffusion equation, we need to consider the boundary conditions.[20] In this study, the probe works in a reflective mode. Hence the semi-infinite boundary condition should be taken into account. The time-resolved TPSF measurements from the breast can be approximated using the difference between the Green's functions respectively induced by an interpolated *real* light source and an extrapolated *image* light source.[18–20] To calculate the optical properties (μ_a and μ_s') from the TPSF measurements, the fitting procedure starts with a reasonable initial estimate $p_0^{\lambda 1,\lambda 2}=[\mu_{a0}^{\lambda 1,\lambda 2},\mu_{s0}^{\lambda 1,\lambda 2\prime}]=[0.03\ \mathrm{cm}^{-1},8.0\ \mathrm{cm}^{-1}]$ for wavelength $\lambda 1=785$ nm and $\lambda 2=808$ nm (Ref. 4). The TPSF prediction R_{pre} was computed from these given estimates. Meanwhile, the TPSF measurements R_m were acquired from the breast tissue. A merit function, defined by $r_i^2=\Sigma(R_m-R_{pre})^2$, is iteratively computed until it meets the convergence criteria $|r_i^2-r_{i-1}^2|/r_{i-1}^2<T_{conv}$, where T_{conv} is a predefined convergence threshold, and i is the iteration number. The initial estimate $p_0^{\lambda 1,\lambda 2}$ was iteratively updated in a step of $p_i^{\lambda 1,\lambda 2}=p_{i-1}^{\lambda 1,\lambda 2}+C\cdot\Delta r_{(i,i-1)}^2$, where C is a step size, and $\Delta r_{(i,i-1)}^2$ is the difference between two consecutive iterations.

The optical properties of human breast tissues are governed by its constituents such as lipid, water, as well as the significant chromophores, HbO and Hb. In this study, we assumed the wavelength-dependent absorption coefficients of the bulky breast tissue were solely contributed by these four types of chromophores: water, lipid, HbO, and Hb. Then, we have

$$\begin{pmatrix} \mu_a^{785} \\ \mu_a^{808} \end{pmatrix} = 2.303 \cdot \left[\begin{pmatrix} \varepsilon_{Hb}^{785} & \varepsilon_{HbO}^{785} \\ \varepsilon_{Hb}^{808} & \varepsilon_{HbO}^{808} \end{pmatrix} \cdot \begin{pmatrix} C_{Hb} \\ C_{HbO} \end{pmatrix} + \begin{pmatrix} \varepsilon_{H_2O}^{785} \\ \varepsilon_{H_2O}^{808} \end{pmatrix} \cdot C_{H_2O} + \begin{pmatrix} \varepsilon_{Lipid}^{785} \\ \varepsilon_{Lipid}^{808} \end{pmatrix} \cdot C_{Lipid} \right], \quad (1)$$

where μ_a^{785} and μ_a^{808} are absorption coefficients of overall breast tissue at wavelength 785 nm and 808 nm, respectively. ε_{Hb}^{785} ε_{Hb}^{808}, ε_{HbO}^{785}, and ε_{HbO}^{808} are molar extinction coefficients of Hb and HbO at 785 nm and 808 nm. $\varepsilon_{H_2O}^{785}$ and $\varepsilon_{H_2O}^{808}$ are molar extinction coefficients of water at 785 nm and 808 nm. $\varepsilon_{Lipid}^{785}$ and $\varepsilon_{Lipid}^{808}$ are molar extinction coefficients of lipid at 785 nm and 808 nm. Their values can be found in the literature.[21] C_{Hb} and C_{HbO} stand for the unknown concentrations of Hb and HbO, respectively. C_{H_2O} and C_{Lipid} stand for the concentrations of water and lipid, respectively. In this study, we assumed and maintained typical values for the relative concentration of lipid (56%) and the water concentrations of postmenopausal (11%) and premenopausal women (26%).[4,11] Given the time-resolved TPSF measurements at 785 nm and 808 nm, values of μ_a^{785} and μ_a^{808} can be resolved by curve-fitting processing. The physiological parameters C_{Hb} and C_{HbO} can be resolved simultaneously by inverting Eq. (1). Value of total hemoglobin concentration (THC) can be obtained by[11,22]

$$THC = C_{HbO} + C_{Hb}, \quad (2)$$

and value of blood oxygenation saturation (SO) can be obtained by

$$SO = \frac{C_{HbO}}{THC} \times 100\,\% = \frac{C_{HbO}}{C_{HbO} + C_{Hb}} \times 100\,\%. \quad (3)$$

Parameter THC has a unit of micromole per liter (μMol/L). It can be interpreted as the blood volume in the breast tissue, from which one can assess the tissue's blood supply. Parameter SO can be interpreted as the degree of oxygen consumption by the breast tissue. Cancerous tissue normally requires much more blood and oxygen supply, which significantly alters the positional optical properties and the physiological parameters of breast tissue. Thus, positional inhomogeneities of μ_a, μ_s', THC, and SO may indicate the presence of breast tissue abnormities.

2.3 *Measurement Protocol*

The *in vivo* breast tissue measurements using the time-resolved DOS instrument have been approved by the Institute Review Board of National University of Singapore. Consent from all volunteer subjects was obtained. Subjects were measured in a sitting posture without any compressions on the breast. The handheld probe was placed on the left and right breasts, respectively, and the positions on each breast are at 3, 6, 9, and 12 o'clock, as shown in Fig. 3. For each wavelength at each position, 36 TPSF measurements were acquired by scanning nine source fibers and four detectors. Each scan took approximately 5 s. In this period, the volunteer was asked to hold her breath. To minimize measurement error caused by heart beating effects of subjects, scanning at each position was repeated 5 times. Thus for each subject, the time-resolved measurements contained $2 \times 8 \times 5 \times 36 = 2880$ TPSFs, which can be obtained in 10 to 15 min.

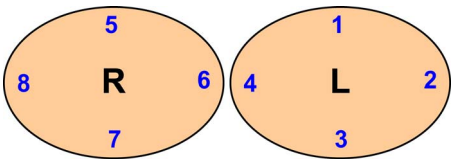

Fig. 3 Probing positions on the left (L) and the right (R) breasts (front view).

2.4 *Subjects*

A total number of 19 Singapore women were recruited for this spectroscopy research. All subjects were healthy without known breast diseases. They were divided into groups according to their menopausal states and age because both aging and menopause states are strongly associated with the replacement of glandular tissue with fatty tissue. The ages of 3 postmenopausal (Post) women were 44, 48, and 50 years. The ages of the remaining 16 premenopausal (Pre) women ranged from 25 to 50 years five women were younger than 40 years, and the remaining 14 women were older than 40 years. The youngest and oldest women subjects were 23 and 50 years old, respectively. Table 1 summarizes the statistics of women subjects by ages and menopausal states. The averaged (Mean) age of all subjects was 41.7 years, and the standard deviation (SD) was 11.1 years.

3 Results and Discussions

The TPSFs obtained from source-to-detector separation of 2.35 cm were selected to calculate the optical properties (μ_a and μ_s'), because this separation allows the incident photons to reach as deep as centimeters into the breast tissue.[11] The

Table 1 Statistics of 19 volunteer women subjects.

	Age		Menopausal states	
	Young (<40)	Older (≥40)	Pre-	Post-
Number of subjects	5	14	16	3
Mean (years)	24.2	47.9	40.8	47.0
SD (years)	1.6	2.8	11.4	2.6
Mean of all (years)		41.7		
SD of all (years)		11.1		

Table 2 Optical properties and physiological parameters of 19 healthy subjects.

Wavelength (nm)	785	808
μ_a (cm^{-1})	0.0503±0.0151	0.0518±0.0153
μ_s' (cm^{-1})	10.53±1.20	10.49±1.19
SO (%)	64.8±10.3	
THC (μMol/L)	22.3±7.5	

calculation of μ_a, μ_s', *THC*, and *SO* were conducted in MATLAB. For each subject, the optical and physiological results at 8 probing positions $R(i)=[\mu_a(i),\mu_s'(i),THC(i),SO(i)]$ $(i=1,\ldots,8)$ were averaged to minimize the interposition variations. Results were expressed by (mean value ± standard deviations). The mean values of μ_a, μ_s', *THC*, and *SO* were regarded as the representative parameters of the entire breast, and the standard deviations were regarded as the interposition variations.

Table 2 summarizes the optical properties and physiological parameters of 19 subjects. The mean μ_a of 19 subjects was found to be 0.0503 cm^{-1}, with a standard deviation of 0.0151 cm^{-1} when a laser wavelength of 785 nm was used while that was (0.0518 ± 0.0153) cm^{-1} at 808 nm. The reduced scattering coefficient showed similarly close results between two different laser wavelengths, with 785 nm showing (10.53 ± 1.19) cm^{-1} and 808 nm showing (10.49 ± 1.17) cm^{-1}. The blood oxygenation saturation (*SO*) of 19 subjects was found to be (64.8 ± 10.3)%, while the total hemoglobin concentration (*THC*) was (22.3 ± 7.5) μMol/L.

In order to investigate the relationship between menopausal states and the optical/physiological parameter, 3 postmenopausal (Post) women and the 16 premenopausal (Pre) women were examined sequentially. Figure 4 shows a scatter plot of μ_s' versus μ_a of 16 premenopausal women (solid blue circles for 785 nm and open blue circles for 808 nm) and 3 postmenopausal women (solid red squares for 785 nm and open red squares for 808 nm) at two wavelengths. The 2-D error bars show the standard deviations of two optical parameters. It was found that μ_s' and μ_a of postmenopausal women are generally smaller than that of premenopausal women, which agreed with the observations in the literature.[22] Statistical results in Table 3 show that the averaged μ_a of premenopausal women was (0.0541 ± 0.0141) cm^{-1} at 785 nm—approximately 60% larger than that of premenopausal women at (0.0338 ± 0.0044) cm^{-1}. At 808 nm, μ_a shows a similar trend of being larger in premenopausal women at (0.0557 ± 0.0141) cm^{-1}—and approximately 61% higher than that of postmenopausal women, which was found to be (0.0347 ± 0.0041) cm^{-1}. The difference of μ_s' between 785 nm and 808 nm is not significant. At 785 nm, the μ_s' of premenopausal women was found to be (10.75 ± 1.17) cm^{-1} on average, which was approximately 12% larger than that of postmenopausal women at (9.6 ± 0.83) cm^{-1}. At 808 nm, the contrast is similar. The μ_s' of premenopausal women is about 12% larger than that of postmenopausal women.

Table 3 Statistics of optical properties and physiological parameters of postmenopausal women and premenopausal women.

	Postmenopausal		Premenopausal	
	Mean	Standard deviation	Mean	Standard deviation
μ_a at 785 nm (cm^{-1})	0.0338	0.0044	0.0541	0.0141
μ_a at 808 nm (cm^{-1})	0.0347	0.0041	0.0557	0.0141
μ_s' at 785 nm (cm^{-1})	9.60	0.83	10.75	1.17
μ_s' at 808 nm (cm^{-1})	9.54	0.81	10.70	1.14
SO (%)	61.6	9.8	65.1	10.3
THC (μMol/L)	14.3	2.3	24.1	7.1

Figure 5 shows a scatter plot of *THC* versus *SO*, which was derived from μ_a according to Eq. (2) and Eq. (3). It is

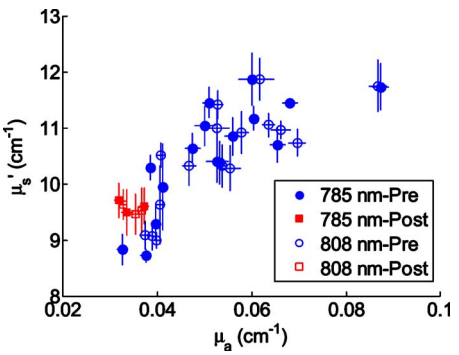

Fig. 4 μ_s' vs μ_a for 19 subjects at two wavelengths. Solid and open red squares represent the results of postmenopausal women subjects at 785 and 808 nm, respectively. Solid and open blue circles represent the results of premenopausal women subjects at 785 nm and 808 nm, respectively. 2-D error bars represent the standard deviation among eight probing positions of each subject. (Color online only.)

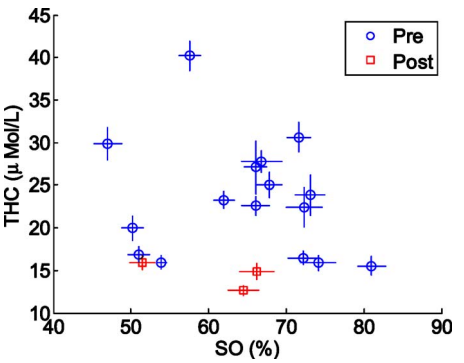

Fig. 5 *THC* vs *SO* for all 19 subjects. Red squares represent the results of postmenopausal women subjects. Blue circles represent the results of premenopausal women subjects. 2-D error bars represent standard deviation among eight probing positions of each subject. (Color online only.)

Table 4 Mean and standard deviation (SD) of optical properties and physiological parameters of 19 subjects. The parameters are compared by age above 40 and below 40 years old.

	Older (age ⩾ 40)		Young (age < 40)	
	Mean	SD	Mean	SD
μ_a at 785 nm (cm^{-1})	0.0447	0.0122	0.0617	0.0143
μ_a at 808 nm (cm^{-1})	0.0462	0.1261	0.0631	0.1392
μ_s' at 785 nm (cm^{-1})	10.154	1.103	11.307	1.010
μ_s' at 808 nm (cm^{-1})	10.108	1.077	11.268	0.987
SO (%)	64.7	11.4	63.8	7.6
THC (μMol/L)	19.6	6.1	27.9	7.0

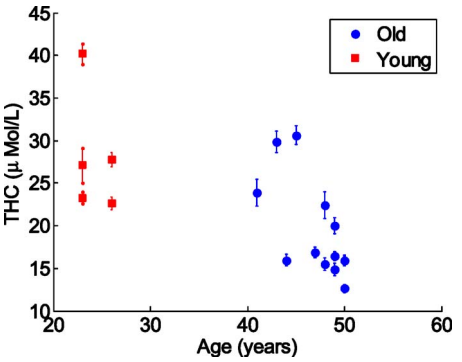

Fig. 7 Scatter plot of parameter *THC* vs ages among all 19 subjects. Red squares represent data of young women, while blue circles represent data of older women groups. Error bars represent the standard deviation of *THC*. (Color online only.)

also clear that the *THC* of premenopausal women, in general, is higher than that of postmenopausal women. Table 3 shows that the *THC* of premenopausal women is (24.1 ± 7.1) μMol/L, which is approximately 69% larger than that of postmenopausal women, which is (14.3 ± 2.3) μMol/L. The *SO* difference between the postmenopausal women and premenopausal women is not significant.

The age of all 19 subjects in this study was (41.7 ± 11.1) years old. To analyze the relationship between age and optical/physiological alterations, subjects are divided into two groups by age over or below 40 (see Table 1). The young women group has 5 women subjects, with ages of (24.2 ± 1.6) years old. The older women group has 14 women subjects, with ages of (47.9 ± 2.8) years old.

Table 4 summarizes the averaged optical properties and physiological parameters in terms of age. Significant contrast between two groups can be found in absorption coefficient (μ_a) and total hemoglobin concentration (*THC*). The μ_a of the young women group at 785 nm was found to be (0.0617 ± 0.0143) cm^{-1}, which is approximately 38% larger than the older women group, in which the averaged μ_a was found to be (0.0447 ± 0.0122) cm^{-1}. At 808 nm, the μ_a of the young women group is (0.0631 ± 0.1392) cm^{-1}, which is approximately 36% larger than that of the older women group at (0.0462 ± 0.1261) cm^{-1}. The higher μ_a values associated with the young women group may be explained by the greater content of fibroglandular tissue in the mammographically dense breasts. Similar difference can also be found in the physiological parameter *THC*. The young women group shows *THC* at (27.9 ± 7.0) μMol/L, while the older women group shows *THC* at (19.6 ± 6.1) μMol/L. The former is approximately 42% larger than the latter. The difference of reduced scattering coefficients μ_s' between the two groups is not significant. The young women group shows an average μ_s' of (11.307 ± 1.010) cm^{-1} at 785 nm and (11.268 ± 0.987) cm^{-1} at 808 nm. Both are approximately 11% larger than that of the older women group. The parameter of *SO* between the young women group and older women group is (63.8 ± 7.6)% versus (64.7 ± 11.4)%. Values are almost same. Figure 6 shows a scatter plot of μ_a among young and older women groups. Figure 7 shows a scatter plot of *THC* among young and older women. For easy comparison, data of the young women group are shown in red squares, and data of the older women group are plotted as blue circles. The error bar shows the standard deviation on corresponding parameters.

In order to examine the correlation between the optical and physiological parameters and women's age, menopausal states, and BMI, correlation analysis using Pearson's correla-

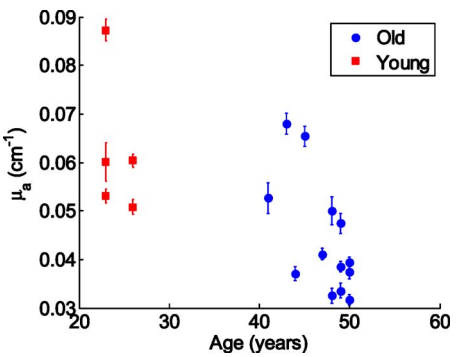

Fig. 6 Scatter plot of μ_a vs ages among all 19 subjects. Red squares represent data of young women, while blue circles represent data of older women groups. Error bars represent the standard deviation of μ_a. (Color online only.)

Table 5 Pearson's correlation coefficient between optical and physiological parameters and subject characteristics.

	μ_a	μ_s'	*SO*	*THC*
Age	−0.6245[a]	−0.6590[a]	0.0609[c]	−0.6294[a]
BMI	−0.5059[b]	−0.5245[b]	0.2427[c]	−0.5097[b]
Menopausal states*	−0.4883[b]	−0.3836[c]	−0.1485[c]	−0.4720[b]

* 0 for premenopausal women; 1 for postmenopausal women.
[a] $p < 0.005$;
[b] $p < 0.05$;
[c] $p < 0.1$.

Table 6 Comparison of optical/physiological parameters from this study and recent literatures. *N* refers to the number of subjects involved in different studies, while μ_s' and μ_a are rounded properly for consistency.

	N	μ_s' (cm^{-1})	μ_a (cm^{-1})	*SO* (%)	*THC* (μMol/L)
Durduran (Ref. 4)	52	9±2	0.04±0.03	68±8	34±9
Grosenick (Ref. 24)	28	10±2	0.04±0.01	74±3	17±8
Tomas (Ref. 26)	36	8±2	0.04±0.02	77±8	17±10
Spinelli (Ref. 27)	>50	11±2	0.04±0.01	66±9	16±5
Taroni (Ref. 28)	101	11±1	0.05±0.01	71±8	20±7
Pogue (29)	46	10±2	0.05±0.04	61±1	22±7
Poplack (Ref. 30)	23	12±2	0.05±0.02	69±9	24±12
Suzuki (Ref. 25)[a]	30	9±1	0.05±0.01	—	—
This study	19	10±1	0.05±0.02	65±10	22±8

[a]Data was obtained using wavelength at 753 nm.

tion coefficients and the Student's *t*-test was conducted. The results in Table 5 show that there is a high and significant correlation between the optical properties of μ_a and μ_s' and women's age, BMI, and menopausal states in a sequence from high to low. The physiological parameter *THC* also shows close relationship with women's age, BMI, and menopausal state as well. The correlation between age, BMI, and menopausal states and the parameter *SO* is low and not significant.

The *in vivo* optical spectroscopy on bulk breast tissues has been investigated worldwide. However, there are subtle differences between results reported from each research group. The differences can be ascribed to the constitutional difference of women subjects (ages, menopausal states, races, and so on), different methodologies and apparatus, and different laser wavelengths used. Table 6 compiles some recent research results on healthy breast tissue using different spectroscopy techniques.[23] All data are rounded properly for comparison. For example, for examinations on Caucasian women, Durduran et al.[4] reported the μ_a of (0.04 ± 0.03) cm^{-1} and μ_s' of (9 ± 2) cm^{-1} at 780 nm from *in vivo* experiments on 52 healthy women. Results reported by Pogue et al.[24] showed a slight difference. The averaged μ_a and μ_s' were (0.05 ± 0.04) cm^{-1} and (10 ± 2) cm^{-1}, respectively. Besides the difference in optical parameters, the physiological parameter results between each group are also slightly different. The average value of *SO* ranges from 61% to 77% and the *THC* ranges from 16 μMol/L to 34 μMol/L. For the study on Asian women, few reports have been published so far. Suzuki[25] reported that the average μ_a from 30 Japanese women was (0.05 ± 0.01) cm^{-1} and the average μ_s' was (9 ± 2) cm^{-1}. In our study, only Southeast Asian women were examined, and the mean values of the optical properties and physiological parameters, as shown in Table 6, showed a good agreement with the data of Caucasian women as well as other regional Asian women.

4 Conclusions

In conclusion, we investigated the range of the optical properties and physiological parameters of breast tissues from 19 healthy Singapore women for the first time. The experiments results show a high correlation between the optical properties (μ_a and μ_s'), physiological parameters (*THC*), and the ages, menopausal states, and BMI of women. The results can serve as a benchmark for diseased breast tissue study in near future.

Acknowledgments

This work was supported by Office of Life Science (R397-000-615-712), National University of Singapore, and research funding support from A*STAR/SERC (P-052 101 0098), Singapore.

References

1. B. Chance, S. Nioka, J. Kent, K. McCully, M. Fountain, R. Greenfeld, and G. Holtom, "Time-resolved spectroscopy of hemoglobin and myoglobin in resting and ischemic muscle," *Anal. Biochem.* **174**(2), 698–707 (1988).
2. B. J. Tromberg, N. Shah, R. Lanning, A. Cerussi, J. Espinoza, T. Pham, L. Svaasand, and J. Butler, "Non-invasive *in vivo* characterization of breast tumors using photon migration spectroscopy," *Neoplasia* **2**, 26–40 (2000).
3. A. Cerussi, N. Shah, D. Hsiang, A. Durkin, J. Butler, and B. J. Tromberg, "*In vivo* absorption, scattering, and physiologic properties of 58 malignant breast tumors determined by broadband diffuse optical spectroscopy," *J. Biomed. Opt.* **11**(4), 044005–044016 (2006).
4. T. Durduran, R. Choe, J. Culver, L. Zubkov, M. Holboke, J. Giammarco, B. Chance, and A. Yodh, "Bulk optical properties of healthy female breast tissue," *Phys. Med. Biol.* **47**, 2847–2861 (2002).
5. S. J. Glick, "Breast CT," *Annu. Rev. Biomed. Eng.* **9**(1), 501–526 (2007).
6. V. Ntziachristos, A. G. Yodh, M. D. Schnall, and B. Chance, "MRI-guided diffuse optical spectroscopy of malignant and benign breast lesions," *Neoplasia* **4**(4), 347–354 (2002).
7. Q. Zhu, N. Chen, and S. H. Kurtzman, "Imaging tumor angiogenesis by use of combined near-infrared diffusive light and ultrasound," *Opt. Lett.* **28**(5), 337–339 (2003).

8. M. J. Holboke, B. J. Tromberg, X. Li, N. Shah, J. Fishkin, D. Kidney, J. Butler, B. Chance, and A. G. Yodh, "Three-dimensional diffuse optical mammography with ultrasound localization in a human subject," *J. Biomed. Opt.* **5**(2), 237–247 (2000).
9. N. Ghosh, S. K. Mohanty, S. K. Majumder, and P. K. Gupta, "Measurement of optical transport properties of normal and malignant human breast tissue," *Appl. Opt.* **40**(1), 176–184 (2001).
10. L. C. Enfield, A. P. Gibson, N. L. Everdell, D. T. Delpy, M. Schweiger, S. R. Arridge, C. Richardson, M. Keshtgar, M. Douek, and J. C. Hebden, "Three-dimensional time-resolved optical mammography of the uncompressed breast," *Appl. Opt.* **46**(17), 3628–3638 (2007).
11. B. Tromberg, A. Cerussi, N. Shah, M. Compton, A. Durkin, D. Hsiang, J. Butler, and R. Mehta, "Diffuse optics in breast cancer: detecting tumors in pre-menopausal women and monitoring neoadjuvant chemotherapy," *Breast Cancer Res.* **7**(6), 279–285 (2005).
12. F. Gao, H. Zhao, and Y. Yamada, "Improvement of image quality in diffuse optical tomography by use of full time-resolved data," *Appl. Opt.* **41**(4), 778–791 (2002).
13. J. C. Hebden, S. R. Arridge, and A. P. Gibson, "Recent advances in diffuse optical imaging," *Phys. Med. Biol.* **50**, R1–R43 (2005).
14. F. E. W. Schmidt, M. E. Fry, E. M. C. Hillman, J. C. Hebden, and D. T. Delpy, "A 32-channel time-resolved instrument for medical optical tomography," *Rev. Sci. Instrum.* **71**(1), 256–265 (2000).
15. S. R. Arridge, J. C. Hebden, and T. D. David, "Optical imaging in medicine: I. Experimental techniques," *Phys. Med. Biol.* **42**, 825–840 (1997).
16. W. Mo and N. Chen, "Fast time-domain diffuse optical tomography using pseudorandom bit sequences," *Opt. Express* **16**(18), 13643–13650 (2008).
17. W. Mo and N. Chen, "Source stabilization for high quality time-domain diffuse optical tomography," in *Design and Quality for Biomedical Technologies II*, R. Raghavachari and R. Liang, Eds., *Proc. SPIE* **7170**, 71700N (2009).
18. R. C. Haskell, L. O. Svaasand, T. T. Tsay, T. C. Feng, M. S. McAdams, and B. J. Tromberg, "Boundary conditions for the diffusion equation in radiative transfer," *J. Opt. Soc. Am. A* **11**(10), 2727–2741 (1994).
19. M. S. Patterson, B. Chance, and B. C. Wilson, "Time-resolved reflectance and transmittance for the noninvasive measurement of tissue optical properties," *Appl. Opt.* **28**(12), 2331–2336 (1989).
20. N. G. Chen and J. Bai, "Monte Carlo approach to modeling of boundary conditions for the diffusion equation," *Phys. Rev. Lett.* **80**, 5321–5324 (1998).
21. S. Prahl, "Optical properties spectra," http://omlc.ogi.edu/spectra/hemoglobin/index.html, (2001).
22. N. Shah, A. Cerussi, C. Eker, J. Espinoza, J. Butler, J. Fishkin, R. Hornung, and B. Tromberg, "Noninvasive functional optical spectroscopy of human breast tissue," *Proc. Natl. Acad. Sci. U.S.A.* **98**(8), 4420–4425 (2001).
23. D. R. Leff, O. J. Warren, L. C. Enfield, A. Gibson, T. Athanasiou, D. K. Patten, J. Hebden, G. Z. Yang, and A. Darzi, "Diffuse optical imaging of the healthy and diseased breast: A systematic review," *Breast Cancer Res. Treat.* **108**(1), 9–22 (2008).
24. D. Grosenick, K. T. Moesta, H. Wabnitz, J. Mucke, C. Stroszczynski, R. Macdonald, P. M. Schlag, and H. Rinneberg, "Time-domain optical mammography: initial clinical results on detection and characterization of breast tumors," *Appl. Opt.* **42**(16), 3170–3186 (2003).
25. K. Suzuki, Y. Yamashita, K. Ohta, M. Kaneko, M. Yoshida, and B. Chance, "Quantitative measurement of optical parameters in normal breasts using time-resolved spectroscopy: *in vivo* results of 30 Japanese women," *J. Biomed. Opt.* **1**, 330–334 (1996).
26. S. Tomas, J. Swartling, P. Taroni, A. Torricelli, P. Lindblom, C. Ingvar, and S. A. Engels, "Characterization of normal breast tissue heterogeneity using time-resolved near-infrared spectroscopy," *Phys. Med. Biol.* **50**, 2559–2571 (2005).
27. L. Spinelli, A. Torricelli, A. Pifferi, P. Taroni, G. M. Danesini, and R. Cubeddu, "Bulk optical properties and tissue components in the female breast from multiwavelength time-resolved optical mammography," *J. Biomed. Opt.* **9**, 1137–1142 (2004).
28. P. Taroni, G. Danesini, A. Torricelli, A. Pifferi, L. Spinelli, and R. Cubeddu, "Clinical trial of time-resolved scanning optical mammography at 4 wavelengths between 683 and 975 nm," *J. Biomed. Opt.* **9**(3), 464–473 (2004).
29. B. W. Pogue, S. Jiang, H. Dehghani, C. Kogel, S. Soho, S. Srinivasan, X. Song, T. D. Tosteson, S. P. Poplack, and K. D. Paulsen, "Characterization of hemoglobin, water, and NIR scattering in breast tissue: analysis of intersubject variability and menstrual cycle changes," *J. Biomed. Opt.* **9**(3), 541–552 (2004).
30. S. P. Poplack, K. D. Paulsen, A. Hartov, P. M. Meaney, B. W. Pogue, T. D. Tosteson, M. R. Grove, S. K. Soho, and W. A. Wells, "Electromagnetic breast imaging: average tissue property values in women with negative clinical findings," *Radiology* **231**, 571–580 (2004).